

真实驾驶循环中的发动机电基合成燃料评估

杨棋锐¹, Michel GRILL¹, Cornelius WAGNER¹, Markus MAUL¹,
Andre KULZER²

(1. 斯图加特汽车工程与车辆发动机研究所(FKFS), 斯图加特 70569, 德国; 2. 斯图加特大学汽车工程学院(IFS), 斯图加特 70569, 德国)

摘要: 电基合成燃料(E-Fuels)是实现环境和气候目标的一个重要组成部分。其中C1含氧化合物因其具备清洁燃烧的特性而备受关注,包括氧化亚甲基醚(OME)、碳酸二甲酯(DMC)和甲酸甲酯(MeFo)。为探索新型燃料在内燃机中的潜力,对汽油和柴油燃烧、排放模型进行了优化和扩展。在成功验证和标定模型后,对虚拟测试车辆进行了研究,重点关注燃料的效率潜力、排放水平和经济性。首先,基于现代汽油、柴油和天然气发动机,开发了不同概念的OME和DMC/MeFo发动机;其次,在真实驾驶循环(RDE)中对这些发动机概念在E级乘用车和40t卡车上的应用进行了评估。结果表明,通过调整喷射策略和匹配废气再循环,OME发动机能实现最佳的热效率和极低的排放;混合燃料DMC/MeFo由于高抗爆性,结合先进的发动机技术,能达到接近柴油机的热效率,且发动机复杂性大大降低,这使得DMC/MeFo燃料在重型卡车应用中具有广阔的前景。

关键词: 电基合成燃料;实际驾驶排放;0D/1D仿真;氧化亚甲基醚;碳酸二甲酯;甲酸甲酯

中图分类号: U473

文献标志码: A

E-Fuels: Model-based Evaluation of Engine Potential in Real Driving Cycles

Qirui YANG¹, Michael GRILL¹, Cornelius WAGNER¹,
Markus MAUL¹, Andre KULZER²

(1. Research Institute for Automotive Engineering and Powertrain Systems Stuttgart (FKFS), 70569 Stuttgart, Germany; 2. Institute of Automotive Engineering (IFS), University of Stuttgart, 70569 Stuttgart, Germany)

Abstract: Electricity-based synthetic fuels (E-Fuels) represent an important building block for achieving ambitious environmental and climate targets. The C1 group oxygenates are due to clean combustion properties particularly attractive, including oxymethylene ether (OME), dimethyl carbonate (DMC) and methyl formate (MeFo). In order to fully explore the potential of new fuels in internal combustion engines, the gasoline and

diesel combustion and emission models were optimized and extended. After successful implementation, validation and calibration of the models, investigations are carried out on virtual test vehicles. These focus on efficiency potential, emission formation and economy. In the first step, different engine concepts of OME and DMC/MeFo are developed, each based on modern gasoline, diesel and CNG engines. In the second step, these engine concepts are evaluated for an E-Class passenger car and a 40-ton truck in virtual real driving cycles (RDE). It can be shown that the OME engine realizes the best efficiency and at the same time minimal emissions through adapted injection strategy and intelligent exhaust gas recirculation (EGR). The blended fuel DMC/MeFo represents great efficiency potential thanks to high knock resistance with state-of-the-art engine technologies. The dedicated DMC/MeFo engines approaches the efficiency of diesel engine concepts with significantly less engine complexity, making DMC/MeFo a promising prospect for heavy-duty application.

Key words: electricity-based synthetic fuel (E-Fuel); real driving cycle (RDE); 0D/1D simulation; oxymethylene ether (OME); dimethyl carbonate (DMC); methyl formate (MeFo)

The strict CO₂ reduction targets worldwide require the continuous further development of drive systems. In the future, the aim is to achieve complete elimination of CO₂ emissions in the transportation sector. The increasing requirements for limiting pollutant emissions of vehicles in real driving conditions (RDE) also calls for efficient emission reduction solutions. The introduction of climate-neutral, synthetically produced fuels is expected to

make an essential contribution on the road to climate-neutral mobility. If fuel is produced based on renewable energies during synthesis, an internal combustion engine can be operated in a CO₂-neutral manner. In addition, fuels can be produced with properties tailored to the application. As a result, synthetic fuels can realize low-emission combustion and help reduce pollutant emissions in the transportation sector.

The development of sustainable synthetic fuels is associated with the requirement of optimum use in internal combustion engines. In particular, this includes the prevention of undesirable emissions such as particles, unburned organic components and nitrogen oxides. A dedicated low-emission fuel thus optimally complements the internal engine measures and modern exhaust gas aftertreatment systems. Furthermore, functionality requirements are to be met, such as high energy density, safe handling, and good combustion behavior.

Various preliminary studies^[1-4] show that oxygenated fuels burn with particularly low soot emissions. The so-called C1 fuels, which do not contain C-C bonds, are characterized by even lower soot formation to hardly any than other oxygenates with the same oxygen content and thus offer a high potential as alternative diesel and gasoline fuels. This property enables the previously unattainable engine operating modes (high exhaust gas recirculation, high dynamics, extreme ambient conditions) for low emissions of other pollutant components such as nitrogen oxides.

In order to make statements regarding the suitability in the combustion engine of these fuels and

to be able to assess their engine potentials, simulation models must be adjusted and extended with regard to new fuel properties. Investigations have shown that the use of C1 oxygenates results in significant differences with regard to emissions, combustion properties and material properties. Their effects on the combustion engine have so far only been experimentally investigated at individual operating points. There are thus large gaps in predictive simulation models for the combustion process and emission formation. A comprehensive statement on engine design for the synthetic fuels is not yet feasible.

In the next chapter, the investigated synthetic fuels and virtual test carriers are presented first. Subsequently, the fundamental model development and validation will be discussed in more detail. Based on the established simulation methodology, engine concepts of synthetic fuels are designed for different scenarios of passenger car and truck applications and their potentials regarding efficiency and emission formations are discussed in the last chapters based on engine maps as well as in real driving cycles.

1 Research object and method

From the large number of chemical compounds potentially suitable as fuels, a selection was made in the course of the study on the basis of existing data or analogies, which showed the following substances from the family of C1-oxygenates to be particularly promising: ① oxymethylene ether (OME); ② methyl formate (MeFo); ③ dimethyl carbonate (DMC). See Fig.1.

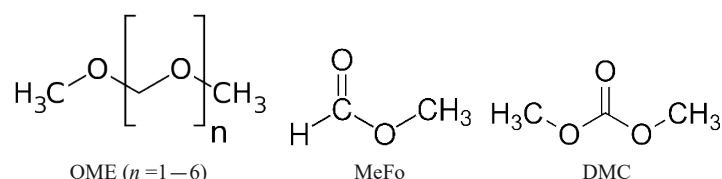


Fig.1 Investigated compound classes

For diesel engines, OMEs have already been identified as potentially sustainable and low-emission fuels^[5-6]. This fuel group has very similar properties to conventional diesel fuel, especially with regard to

handling.

In the area of gasoline fuels, DMC and MeFo are considered. Both fuels are characterized by high knock resistance properties. For this reason, DMC

has already been discussed as an additive for gasoline in the past^[7]. Practical tests^[8] have shown that an improvement of HC and CO emissions can be expected, while hardly any influence on NO_x was observed. With the exception of a patent on blending gasoline with MeFo to improve knock resistance^[9], there is no evidence in the literature for using this particularly volatile oxygenate as an engine fuel beyond basic combustion studies. Since MeFo and DMC have an identical elemental composition (C_nH_{2n}O_n, n=2 and 3), thus have the same gravimetric calorific value and are also similarly knock resistant, their direct comparison in terms of engine combustion and emissions appears interesting. The main difference is in the boiling behavior (boiling point of DMC: 90 °C, MeFo: 32 °C), which is of great importance in the gasoline direct injection process for sufficient homogenization of the mixture.

DMC and MeFo have emission advantages over non-C1 fuels and the advantage of lower health hazards over the C1 oxygenate methanol, which means that optimum acceptance in mobile applications can be expected.

Appropriate fuel properties such as vapour pressure and evaporating behavior must be made for the sake of safe use in both summer and winter. Therefore, reasonable fuel mixtures and blends instead of pure fuels are composed: a liquid mixture of mainly OME₃, OME₄ and OME₅ volumetrically at 57.9% / 28.87% / 10.07% (OME₃₋₅), a binary mixture of DMC and MeFo volumetrically at 65% / 35% (C65F35) and a gasoline blend fuel with 85% of gasoline and 15% of MeFo (G85F15). Tab. 1 shows the properties of the synthetic fuels compared to conventional fuels.

Tab.1 Substance properties of investigated fuels

	Unit	Diesel	OME ₃₋₅	Gasoline	G85F15	C65F35
H/C	—	1.87	2.35 ¹⁾	1.94	1.95	2.08
O/C	—	0	0.82 ¹⁾	0.03	0.08	1
Spec. evaporation enthalpy	kJ/kg	250	350	350	362	433
Spec. heat capacity liquid	J/(kg·K)	2400	2400	2400	1939	1485
Stoichiometric air/fuel ratio	—	14.5	5.91 ¹⁾	13.91	13.01	4.65
Lower heating value H _u	MJ/kg	42.8	19.21 ¹⁾	42.20	38.05	15.20
Density (15 °C)	kg/m ³	830	1057.1 ¹⁾	744	789	1041

1) Values determined in laboratory report.

Although the use of a particular fuel is not limited by the engine class, this study preconceives the primary use of gasoline and diesel alternatives respectively in small engines for passenger car segment and in large engines for heavy-duty sector. A reference passenger car gasoline engine and a heavy-duty diesel engine are chosen: VW EA211evo^[10]; MAN D2676^[11-12].

These two engines serve as a basis for the design of engine concepts for the synthetic fuels. In order to further evaluate the engine performance in real driving conditions, representative vehicles in both segments are chosen: Mercedes E-Klasse^[13]; MAN TGX 18.440^[14-15].

The whole engine design and evaluation was carried out with the aid of 0D/1D simulation, where reliable, predictive simulation models are a mandatory prerequisite. These models must not only

capture the physical influences of the changed fuel properties and possible operating modes on the in-cylinder processes and calorics, but the reaction kinetic influences of the fuels on the combustion process, knock behavior and emission generation must also be reproduced predictively. For this reason, the existing models for conventional diesel and gasoline fuels were optimized and extended for the investigated synthetic fuels in the first place.

2 Modeling synthetic fuels in 0D/1D simulation

The study of the interaction between fuel and engine requires intensive simulation work, which can provide a deep understanding of the system and thus enable cost-effective further developments. The basis

for this is the simulation models. Due to the different operating principles of compression ignition (CI) engines and spark ignition (SI) engines, two sets of simulation models are required. The model development and validation are discussed in this section respectively for the diesel and gasoline-alternatives.

2.1 OME₃₋₅

A diesel equivalent combustion is composed of a series of sub-processes: fuel injection, evaporation, ignition delay, mixture formation, heat release and emission formation. Due to a number of differences that OMEs exhibit from diesel fuel, these sub-processes will change. For example, the heating value of OME is gravimetrically only about half. The start and end of boiling points are at significantly

lower temperatures, the flash point and cetane number are somewhat higher-especially in the case of longer-chain OMEs. OMEs also tend to be less viscous and more diffusive. Last but not least, they have different C/H/O atom ratios and exhibit completely different reaction kinetics. As a result, the fuel injection, mixture preparation, ignition delay and burnout behavior are different between diesel and OME.

The quasi-dimensional combustion model uses a series of sub-models to describe these processes, whose interaction is shown in Fig. 2. The sub-models are studied one by one and adapted to OME. A brief model conception and important model adaptations will be described below.

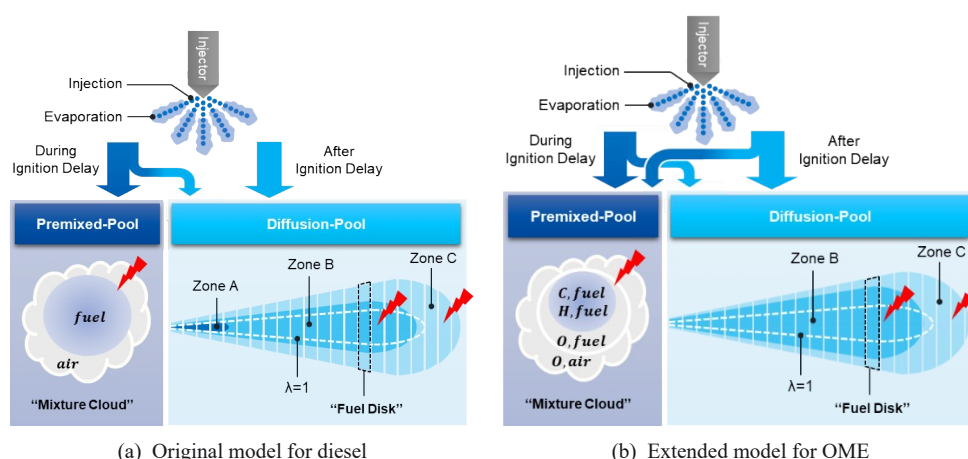


Fig.2 Schematic representation of diesel-equivalent combustion modeling

The modeling of a mixture-controlled combustion is based on the injection process. Within the scope of the study, the injection process is modeled with a common rail system via a polygon course according to Barba^[16]. An OME operation requires almost twice the mass for the same power output as diesel. The vaporization of the fuel following the injection is modeled via a characteristic vaporization time^[17] and describes the time delay between the introduction of liquid fuel and the availability of vaporized fuel for combustion. The higher enthalpy of vaporization of OME is automatically taken into account in the vaporization model.

In the original model conception^[16], each

injection, namely evaporated fuel, is assigned a premixed pool and a diffusion pool. During the ignition delay, the main part of injection is introduced into the premixed pool and forms a fuel-air mixture cloud. The ignition delay is determined here by the turbulent mixing processes according to the Magnussen approach, and by the chemical reaction kinetics according to the Arrhenius approach^[18]. Since the investigated OME mix has a cetane number of 68.6, which is higher than that of diesel with a value of 53.1^[34], this also means a shorter ignition delay from a reaction kinetics point of view^[19]. This property of OME is well represented with a reduction of activation temperature in the Arrhenius term. Furthermore, an adjustment is made that not only the

oxygen from the environment into the air-fuel-mixture is considered, but also the oxygen content of the fuel. At the same time, the fuel concentration only includes the carbon and hydrogen content in the fuel. The oxygen content in the fuel is thus subtracted. These adjustments result in a new formula of the Arrhenius term:

$$r_{Arr} = K_{ID1} \cdot K_{Arr} \cdot C_{HC, fuel} \cdot C_{O, air+fuel} \cdot e^{-\frac{k_f \cdot T_A}{T_m + Q_f \cdot K_{ID2}}} \quad (1)$$

After ignition delay is reached and ignition takes place, the afterwards injected fuel only flows into diffusion pool and burns diffusively. For modeling diffusion combustion, injection spray is temporally and axially locally discretized to multiple fuel disks. Each fuel disk consists of 3 zones, namely: an extremely rich zone A, non-ignitable; a lambda favorable zone B, which burns relatively fast; and a lean zone C, which is mixture controlled and burns relatively slowly. To subdivide these 3 zones, an empirical lambda distribution in the radial direction is specified, which is dependent on the diffusion rate of the fuel-air mixture. This model conception works well for diesel. Adjustments are yet needed for OME. Since OME brings oxygen with it into the combustion chamber, OME can be seen as partially pre-mixed. Out of this consideration, part of OME is assigned to the premixed pool.

Furthermore, OME has a higher diffusion coefficient in the air $D_{fuel/air}$ than diesel, a more homogeneous lambda distribution can be expected in

the OME spray. Both the higher lambda value in the middle of spray and the more homogenous lambda distribution within spray result in more fuel into the diffusion I pool (zone B) that burns quickly.

Using measurement data of diesel and OME on a single-cylinder research engine with a displacement of 533 cm³ and a standard passenger car diesel injection system, pressure trace analysis was performed and the model validated. Tab. 2 shows the variation range of the measured operating points.

Tab.2 Operating range of measurement data for validating the combustion model for diesel and OME

Value	Variation range
Engine speed	1500 1/min
Load	3 bis 10 bar
Combustion center	4–16 °CA after TDC
EGR ratio	0–50%

The results of the combustion modeling can be seen in Fig. 3 and Fig. 4. In the reference diesel cases without EGR, the heat release rates from PTA can be reproduced well by the simulation. Fig. 4 shows the comparison between PTA and the simulated heat release rate with OME. The PTA results are reproduced as well. Even lateral influences such as changed EGR, combustion center and load can be predicted with the model with sufficient quality. Finally, it should be emphasized that the model represents the combustion of diesel and OME with a predominantly identical set of model parameters. The model thus proves to be predictive.

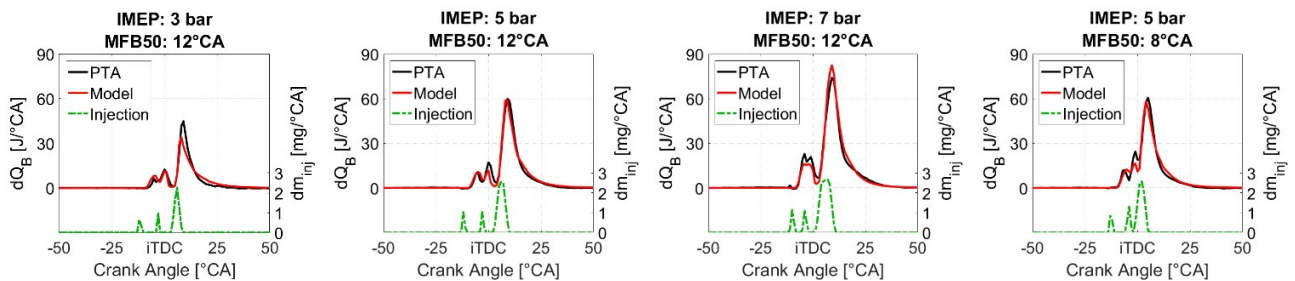


Fig.3 Validation results combustion modeling of diesel

Since the emission behavior is of decisive importance in the diesel engine, the corresponding emission models must be adapted to the changed boundary conditions of an OME combustion in addition to the combustion model. The exiting NOx

and soot emission model^[20-21] proved to be generally applicable to OME. This model is based on the combustion model and the thermodynamic modeling of the combustion chamber into two zones, the unburned and the burned zone. The combustion

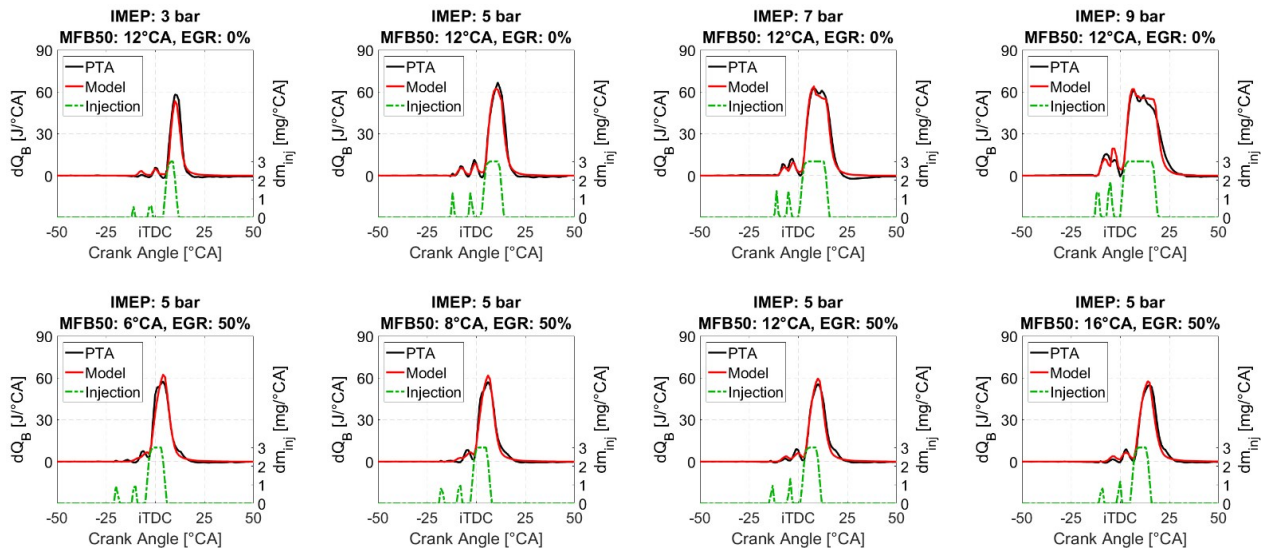


Fig.4 Validation results of combustion modeling of OME

model provides the amount of heat attributed to the burned zone via an adiabatic isobaric change of state. Taking into account the gas caloric, the temperature of the burned zone is thus determined. This serves as input variable of the Zeldovich mechanism, via which the NO emission is calculated. It was shown that the original parameter set of the Zeldovich mechanism predicts NO emissions that are too low, especially at low temperatures.

Due to the higher mass of fuel to be evaporated as well as the possible operation with high EGR ratio for OME, a lower combustion temperature is to be expected, which is why an enhancement of the Zeldovich mechanism became necessary. A new parameter set is therefore found on the basis of detailed reaction mass kinetic calculations, which can

provide more accurate NO calculation in wider boundary conditions of lambda, temperature and pressure.

Fig. 5 and Fig. 6 shows respectively the validation results regarding soot and NO emissions using the measurements as mentioned above. A load variation without EGR, a combustion center variation without EGR, and a combustion center variation with 50% of EGR are shown for each fuel. No measurement data is available for the diesel load variation due to test equipment failure. For the other operating points, soot and NO_x emissions of diesel and OME were met simultaneously by adjusting a limited number of model parameters. A single parameter set was used for diesel and OME respectively. The emission model is thus considered validated.

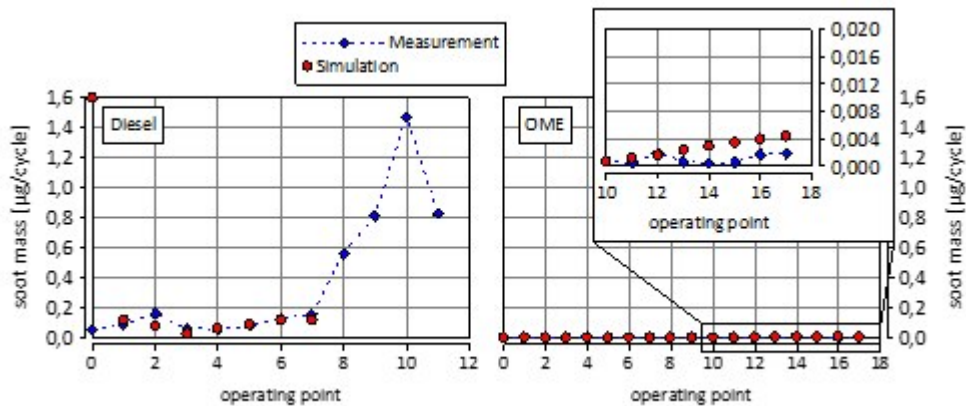


Fig.5 Validation results of soot emission modeling

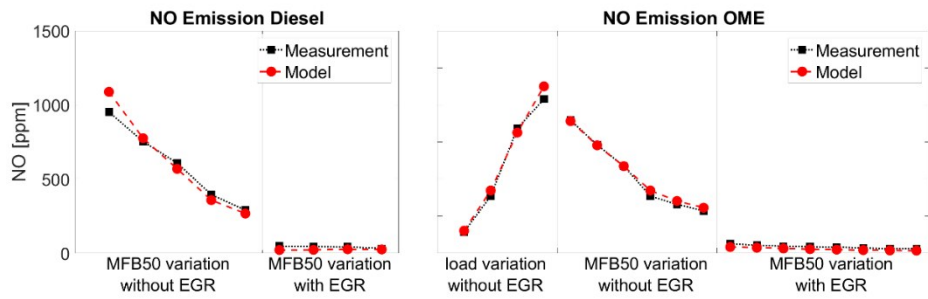


Fig.6 Validation results NO emission modeling

2.2 C65F35 and G85F15

A quasi-dimensional approach^[21-22] is also used for modeling combustion in SI engine. It assumes a hemispherical flame propagation from the spark plug. The combustion chamber is divided into three areas: unburned zone, burned zone and flame front which separates these two zones (Fig. 7). The model first describes a physical process whereby unburned material is carried by flame propagation through the flame zone into the burned zone (flame suction). The flame propagation velocity is positively related to the laminar flame speed and turbulence intensity. A turbulence model is used to determine the charge motion (tumble), its conversion to turbulence as well as the turbulence generation out of fuel injection^[23]. A laminar flame speed model is responsible for the calculation of the laminar flame speed^[24]. These two sub-models must be able to cope with the investigated fuels C65F35 and G85F15. Due to the similarity in the model adjustments for both fuels, C65F35 is used for further explanation.

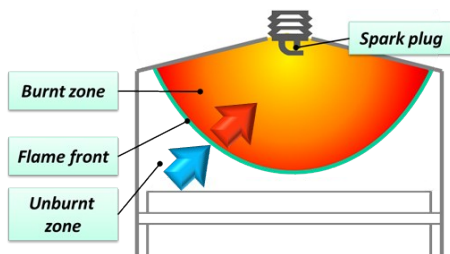


Fig.7 Schematic representation of combustion modeling of SI engine

For the charge motion and turbulence model, it is important to consider the influence of the changed injection mass due to the different calorific value of the fuels. It could be shown that the tumble behavior can be

changed by the injection in the case of a lateral injector position. Since the tumble is converted into turbulence in the course of the piston movement, the injection strategy plays a decisive role for the subsequent combustion process. The model is enhanced to reproduce these influences and validated with 3D CFD simulations. Fig. 8 shows a comparison between 3D CFD and model calculations regarding turbulence kinetic energy (TKE) and tumble value when changing the injection timing (SOI) and the engine speed (RPM) for C65F35. It can be clearly observed that late injection leads to tumble buildup, which makes the level of TKE in the near-combustion region much higher than for the other variants. In the speed variation, the influence of injection with increasing speed does not affect the tumble as much as at low speeds. The model can well reproduce the influence of fuel injection on tumble and turbulence, thus providing a reliable statement about the turbulence level during combustion.

In addition to turbulence, the laminar flame speed plays a decisive role for the burning process. The applied model^[25] follows the approach that the laminar flame speed is defined fuel-specifically and represent itself as functions of pressure, temperature, air-fuel ratio, EGR rate and water content. The model provides a number of tuning parameters to depict these influences on specific fuel. These parameters were derived from the reaction kinetic simulations based on the specific reaction mechanisms for C65F35 and G85F15^[26]. Fig. 9 shows the deviation of the model calculation from the reaction kinetics simulation for C65F35. As an example, engine cycles of two different load points at $\lambda=1$ are shown in the upper part of Fig. 9. The deviations are

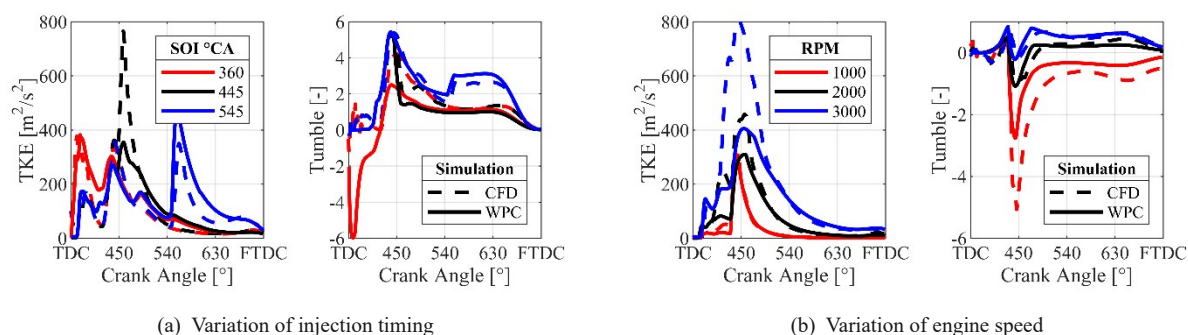


Fig.8 Comparison of TKE and the tumble between 3D CFD and model calculation (WPC)

below 5% in the engine-relevant conditions. A lambda and an EGR variation are shown in the bottom part of Fig. 9. The model yields generally accurate laminar flame speeds in the lambda and EGR variations. The error increases only on the outer edges with a higher EGR and λ , where the conditions are subordinate to the engine application.

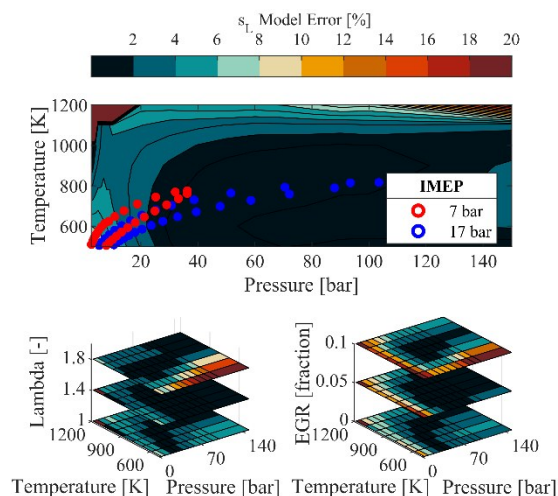


Fig.9 Comparison of TKE and the tumble between 3D CFD and model calculation (WPC)

With the model enhancements for C65F35, the combustion model is now validated with the measurements on a single-cylinder research engine^[27] and a series 4-cylinder engine^[28]. Validations on the characteristic points including idle, load, corner torque and full load are shown in Fig. 10 for the full engine. In general, the combustion processes from PTA are very well matched with the calibrated model with a single parameter set for each engine.

The deviation of the indicated mean pressure between simulation and measurement is less than 5% at all points.

Besides combustion modeling, a reliable knocking prediction is required for the design of virtual engine concepts. This behavior can be simulated by modeling the auto-ignition behavior and further by means of knock prediction through a knock criterium. Since C65F35 is an extremely knock resistant fuel, there is no broad database of knock measurements available. It could be shown on the test bench that with an increase of the intake temperature the engine can be brought to the knock limit. These measurements were used for the calibration and validation of the auto-ignition model. In addition, the knock model was tuned so that a further increase in intake temperature or intake pressure from the knock limit leads to a shift of the combustion center by the knock control toward late.

The extreme potential in terms of NO emission of C65F35 was observed on the test bench^[27]. An emission model is required for the subsequent assessment of NO emissions in engine concept studies. The same NO modeling approach for diesel and OME was used here and validated using test bench data. The agreement of the model with selected load points for a lambda and load variation is shown in Fig. 11. The measurements were carried out on the single-cylinder engine with C65F35. The model agrees very well with the measurements.

3 Design of engine concepts for synthetic fuels

Now that the simulation has been made capable of predicting the behavior of OME, C65F35 and G85F15, engine concepts for practical applications

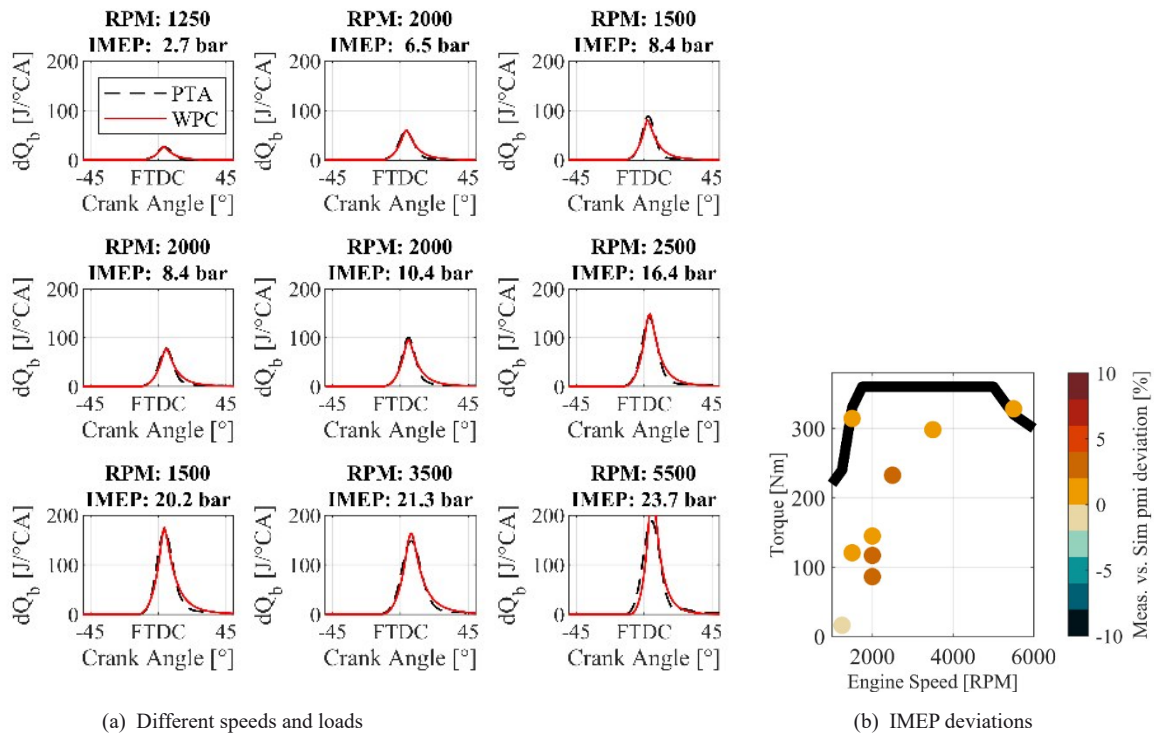


Fig.10 Heat release rates of 4-cylinder engine for different speeds and loads, and IMEP deviations

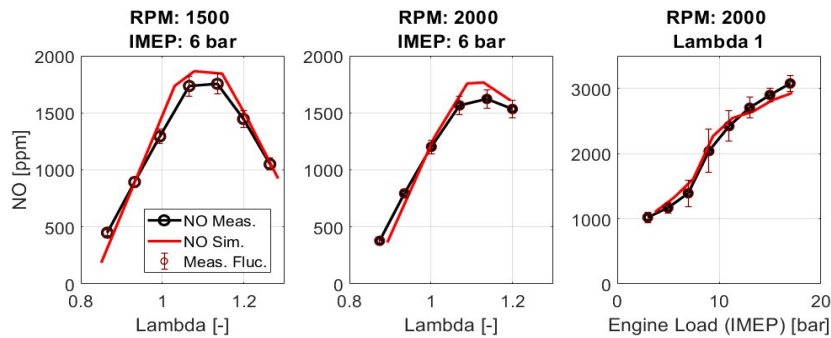


Fig.11 NO Comparison simulation vs. measurement for the fuel C65F35

are developed.

3.1 Passenger car engine concepts with G85F15 and C65F35

The base engine is VW EA211 TSI evo, which is equipped with gasoline direct injection, variable-geometry turbocharger (VGT), variable valve timing with Miller process, a high compression ratio and

cylinder deactivation in part-load. This engine is characterized by a high efficiency over a wide range of the characteristic map and represents the state of the art. Starting from this, different concepts are conceived for the synthetic fuel C65F35 and the gasoline blend fuel G85F15. Tab. 2 gives an overview of the passenger car engine concepts.

Tab.2 Passenger car engine concepts with key technologies

Parameter/Engine type	Base	Cost Optimized	High Efficiency
Fuel	G100, G85F15, C65F35	G85F15, C65F35	G85F15, C65F35
Displacement volume	1 500 ccm	1 000 ccm	1 000 ccm
Compression ratio	12.5	12, 17	11–19, 16.5–19
Lambda	1	1	1–1.4
Valve timing	Variable (Miller)	static	Variable (Miller)
Turbocharger	VGT	VGT	VGT+e-Booster
Cylinder deactivation	Yes	No	Yes

In the first step C65F35 and G85F15 replacing gasoline are directly used in the base engine without changing the engine design. Fig. 12 shows how the change in fuel affects the brake efficiency in the characteristic map for the base engine. With an admixture of 15% MeFo, the knock behavior improves significantly. In the high load range, this leads to an earlier combustion center MFB50 and thus to better efficiency. The same applies to C65F35, with significantly brake efficiency increase

including the low-end-torque area. Meanwhile, the change in fuel brings moderate efficiency losses in lower part-load. This is on the one hand due to the slower laminar flame speed of DMC and MeFo compared to gasoline and thus the longer burn duration, on the other hand due to the higher mixture heating value of G85F15 and C65F35 with air compare to gasoline-air mixture and thus a stronger throttling needed. This fact already suggests the high potential of downsizing.

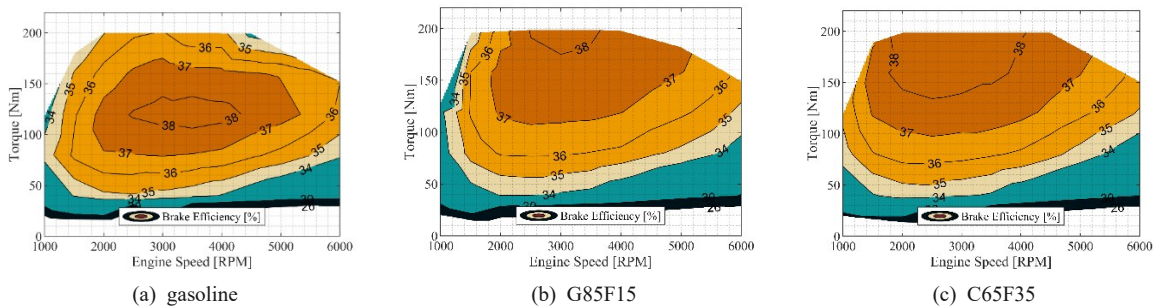


Fig.12 Comparison of characteristic maps of gasoline, G85F15 and C65F35 for base engine

In the second step, a cost-optimized concept and a high-efficiency concept are designed respectively for C65F35 and G85F15. In the former case, the displacement volume is reduced by 500 ml to 1000 ml. At the same time, technologies that make the propulsion system more complex are omitted. This concerns cylinder deactivation and variable valve train. The compression ratio is reduced for G85F15 to operate the engine over wide ranges in the

characteristic map with an optimum combustion center. It is necessary to sacrifice torque in the low-end torque range because the turbocharger does not have enough exhaust gas enthalpy to increase pressure, despite the late combustion center (20° CA) due to knock avoidance. Further retardation of the combustion center can remedy this but at efficiency costs. The area of best efficiencies moves towards the middle of the map, as shown in Fig. 13.

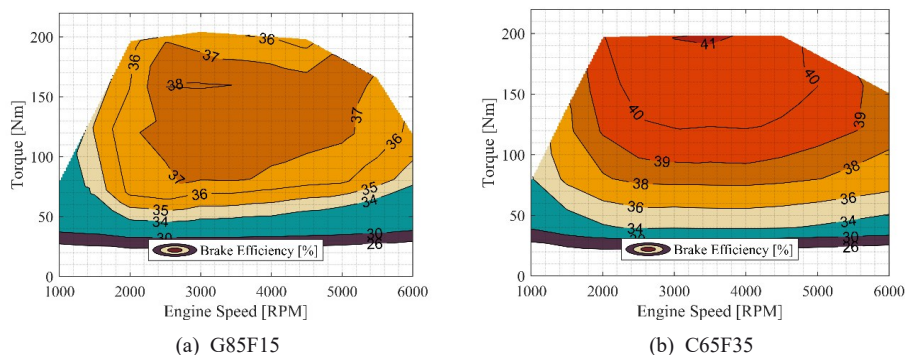


Fig.13 Characteristic map of cost-optimized concepts for G85F15 and C65F35

The peak efficiencies drop slightly due to the tradeoff in valve timing. Nevertheless, a comparison with the gasoline base engine shows that a similar level of efficiency can be maintained using the cost-

optimized concept of G85F15 with significantly less system complexity. In the C65F35 case, the compression ratio can be increased significantly to 17. Again, there are torque losses at low engine speeds

(Fig. 13 (b)). The exhaust gas enthalpy is insufficient to build up the charging pressure since it is possible to operate with an optimum center of combustion in the low-end torque area. The best efficiency of the C65F35 concept reaches a value of 41.1%. This results in a peak pressure of 177 bar at a BMEP of 25 bar. The area of high efficiency extends over the large parts of full-load region down to the medium part-load.

For the high-efficiency concepts, all available technologies are used to achieve the highest possible efficiency. This includes lean combustion strategy, variable compression ratio, variable valve train as well as cylinder deactivation. Due to the low exhaust gas enthalpy in the low-end-torque area caused by downsizing, it is necessary to support the turbocharger e. g. with an e-machine. It was determined in Ref. [35] that measures such as optimized diffuser geometry, bearing resistance reduction, and advanced manufacturing processes will lead to efficiency improvements of turbochargers.

In the G85F15 dedicated high-efficiency concept, a lean combustion with $\lambda=1.4$ is applied to the low load range to benefit from the de-throttling of the engine, see Fig. 14. The rest range

of the characteristic map maintains stoichiometric operation for two reasons. Firstly, the turbocharger reaches its performance limit for higher λ s at high loads.

Although the boost demand can be compensated by the e-turbo, the e-turbo is because of its negative impact on efficiency not overused, but only applied for low-end-torque. Secondly, the G85F15 engine with lean operation becomes prone to knocking at higher loads^[29], leading to a limited range of lean operation. The variable compression ratio is displayed at the top right. At moderate to high engine speeds and low loads, a compression ratio of 19 is applied. A higher compression ratio would be conceivable, but due to geometry limitations, the compression volume gets too small and leaves no space for the spark plug if a flat piston is maintained. At high loads, the compression ratio is successively reduced to 11 due to the increasing knock tendency. At low speeds, a high compression ratio harms brake efficiency. A significantly increased frictional power causes this at high compression ratios. The NO emission is kept below 50 ppm in lean operation. With increasing load and stoichiometric operation, the NO emissions increase strongly.

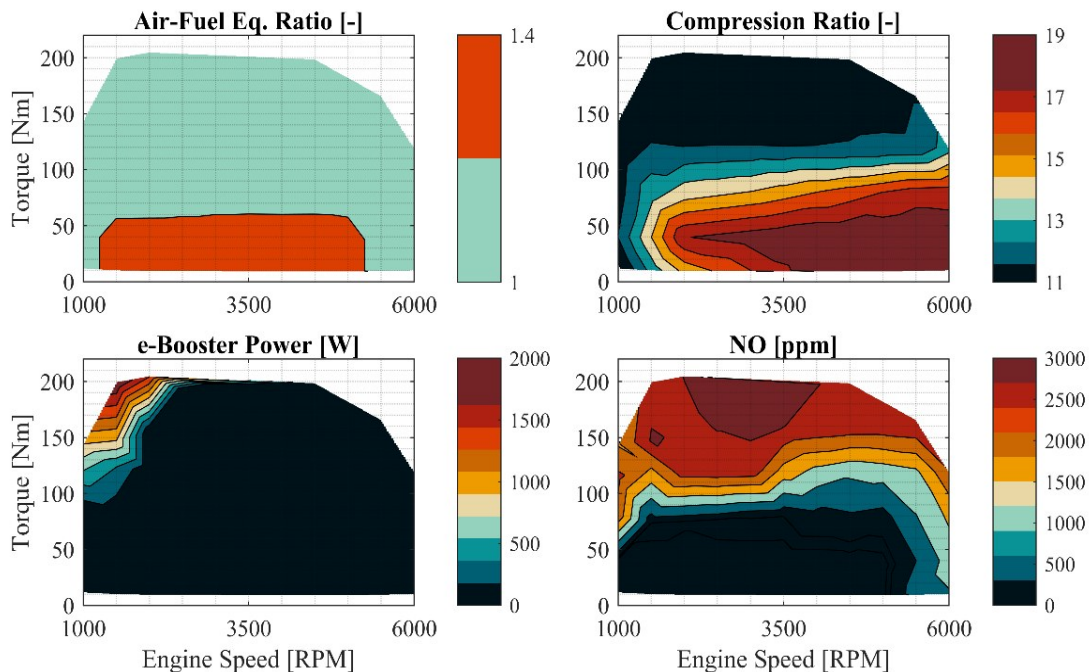


Fig.14 Maps of the G85F15 high-efficiency engine for A/F equivalence ratio (top, left), compression ratio (top, right), e-turbo power (bottom, left), and NO emissions (bottom, right)

In the C65F35 dedicated high-efficiency engine, the lean concept is applied in a considerably wider map range, except for the rated power area where the available boost pressure is limited by the turbocharger. A similar compression ratio strategy is adopted here as the G85F15 engine but with a much higher value at high loads (CR=16.5). It would also be possible to use higher compression ratios in this

area since the combustion center can remain optimal thanks to the high knock resistance of C65F35. However, due to the mechanical limitation of peak pressure in the combustion chamber, the compression ratio is not further increased. A significant benefit of raw NO emission can be observed. The emission value is well below 300 ppm where the lean combustion operates.

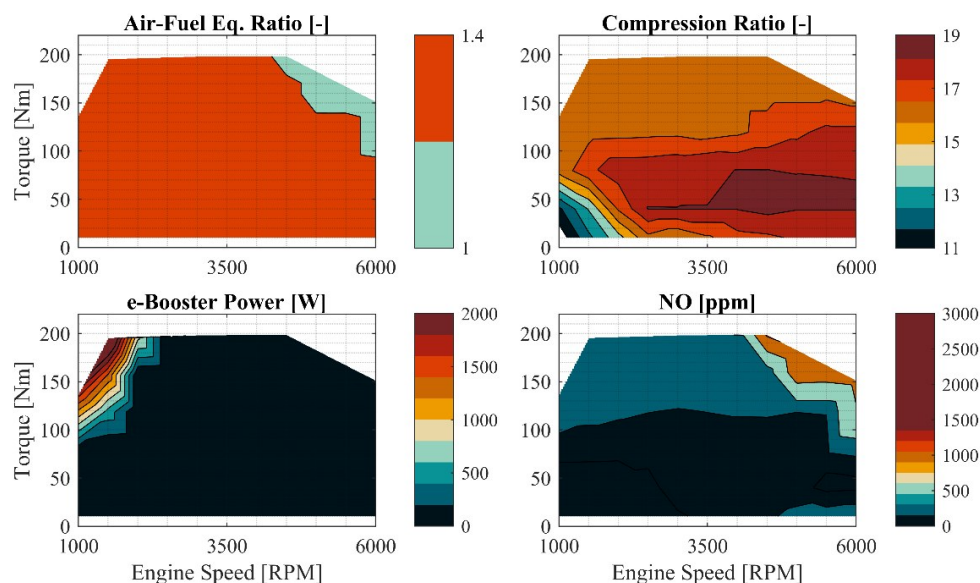


Fig.15 Maps of C65F35 high-efficiency engine for A/F equivalence ratio (top, left), compression ratio (top, right), e-turbo power (bottom, left), and NO emissions (bottom, right)

Both synthetic fuel engines represent now a wide range of high efficiency in the map, extending from lower part-load to full load. The engine design with

C65F35 shows the greatest efficiency potential. A peak efficiency over 42.5% is reached.

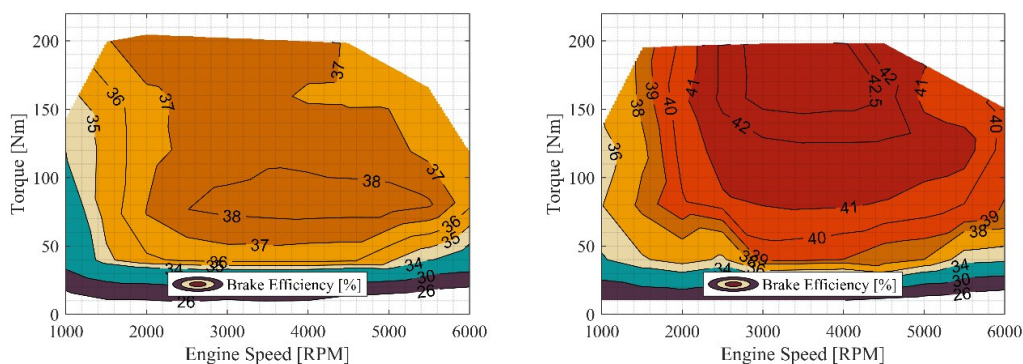


Fig.16 Characteristic map of the high-efficiency concepts for G85F15 (left) and C65F35 (right)

3.1 Commercial vehicle engine concepts with OME and C65F35

Particular attention is now being paid to applications in the commercial vehicle sector, where electrification of the powertrain will obviously quickly

reach its limits. A total of 4 engines for 4 fuels are investigated. An OME-powered engine was developed from a diesel engine, and a C65F35-powered engine from a CNG engine. Tab. 3 lists the engine concepts for comparison.

Tab.3 Truck engine concepts

Parameter / Engine type	Base engine		New concept	
	Fuel	CNG	Diesel	C65F35
Mixture formation	Intake manifold injection	Direct injection	Direct injection	Direct injection
Displacement	12.9 L	12.42 L	11.5 L	12.42 L
Compression ratio	12	17.5	14	17.5
Lambda	1	1.2 - 5.5	1	1.2 - 5.5
Exhaust gas recirculation	internal	external (HP)	internal	external (HP+LP)
Turbocharger number	2	2	1	2

The six-cylinder diesel base engine refers to the MAN engine of series D2676 (displacement: 12.4l, power: 353 kW at 1 900 r·min⁻¹), which is characterized by a two-stage turbocharging, high-pressure common-rail injection up to 1 800 bar, λ -regulated high pressure EGR (HP-EGR) and a modern exhaust after-treatment system. The dimensions and specifications of the engine and exhaust gas aftertreatment were determined from Ref. [14-15] corresponding to the Euro VI emission standards. In the engine design for OME, the following boundary conditions were taken into account for the purpose of a fair comparison with diesel operation:

- The combustion center position is kept the same as for diesel application.
- The maximum cylinder pressure is limited to 193 bar due to component mechanical protection.
- Boost pressure control remains unchanged as with diesel application
- The friction power of the injection system is determined according to injection requirements.

Due to the lower volumetric energy of OME than diesel, more fuel mass is required through the injector for the same power output. The increased pumping power of the fuel system is considered in the simulation, under the simple assumption that an additional friction power of 8 kW is needed to supply OME at the rated-power point. The friction power is modeled to be reduced depending on the fuel mass flow at lower loads and speeds.

The engine design was carried out in 5 stages. In Stage 1, the OME engine has the same hardware as the diesel engine. Due to the lower heating value of OME, longer injection is required at higher loads, which increases the burn duration. This leads to thermodynamic disadvantages and thus to lower

efficiency compared with the diesel engine. At operating points with low to medium loads, the efficiency advantage of faster combustion of OME is counteracted by the increased fuel pumping power consumption. To compensate for the longer burn duration, in Stage 2, the injector is replaced by one with double hydraulic flow. As a result, the burn duration is reduced by a factor of 2 at almost all operating points, thereby increasing efficiency. The faster combustion slightly increases the temperature in the combustion chamber and also increases NO emissions, which are still at the level of the diesel engine. Thanks to the much lower particulate emissions from OME, the EGR rate is increased in Stage 3. Even without geometric changes to the high-pressure EGR path, NO emissions can be greatly reduced across the entire map. The lower charge exchange work also increases the effective efficiency, especially at higher engine speeds. At low speeds, the necessary mass flow can no longer be generated via the turbine, so efficiency decreases here. Using low-pressure EGR instead of high-pressure EGR in Stage 4 shows the opposite behavior. Efficiency increases at low speeds compared to Stage 2, but decreases at higher speeds due to the increased charge exchange work. A combination of high-pressure and low-pressure EGR in Stage 5 results in the OME concept engine. As in Ref. [30], low-pressure EGR is used at low speeds and high-pressure EGR at higher speeds.

Fig. 17 and Fig. 18 compare the diesel and OME engines regarding efficiency and emissions. The OME engine has significantly lower NO and particulate emissions, the higher peak efficiency over 45% and a wide high-efficient area. It is also to be noted that the diesel efficiency drops sharply with increasing engine speed at high loads due to the

increasing combustion duration of longer injection. This is where the OME has advantages thanks to the

faster diffusive combustion, benefiting the real driving application that will be discussed in the next section.

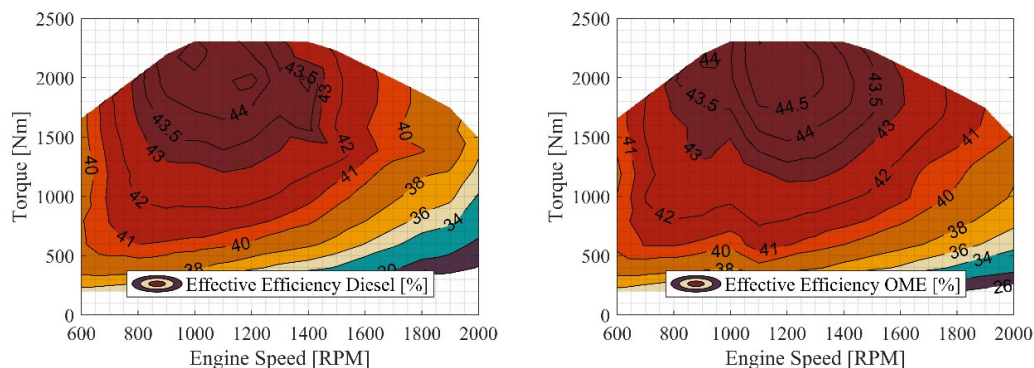


Fig.17 Effective efficiency of diesel (left) and OME engine (right)

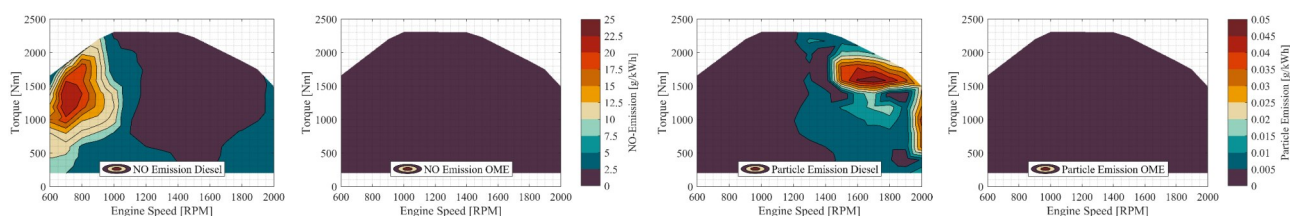


Fig.18 Specific NO and particulate emissions from diesel (left) and OME engine (right)

Since the synthetic fuel C65F35 offers enormous potential for high-efficient engine concepts, as shown in the previous section, it is also brought into play for heavy-duty applications. To estimate the potential of C65F35 for heavy-duty vehicles, a base CNG engine from Ref. [31] is used. Ref. [25] has shown that the combustion model used can represent the fuel conversion from CNG to liquid fuels with high quality. The turbulence level in the combustion chamber is adopted from the base engine. The changes to the base CNG model regarding the new fuel C65F35 are fuel properties, laminar flame speed, ignition delay calculation and knock model and injection concept.

Considering the price sensitivity of the truck segment a cost-optimized concept of C65F35 is developed, which has a moderate downsizing level from the base CNG engine, an increased compression ratio and simple stoichiometric operation. The boost pressure is provided by only one turbocharger, since, compared with the diesel engine, no excess air needs to be ensured in the combustion chamber due to stoichiometric operation. In addition, compared with

the CNG concept, the fuel is injected directly into the combustion chamber, which means that no fuel-air mixture needs to be introduced into the combustion chamber by the turbocharger (See Fig. 19).

The C65F35 engine has significant efficiency advantages over the CNG base engine. Further downsizing of the C65F35 engine would be conceivable. However, the combustion center controller counteracts this due to knock detection. Since no reliable knock measurements have yet been carried out for this engine class and application, the model keeps the conservative assumption regarding the knock behavior of C65F35.

4 Potential evaluation of synthetic fuels in real driving conditions

The evaluation of the engine concepts was carried out in the previous section on individual load points or on the entire engine map. Furthermore, virtual driving cycles can be used to infer the real power and load requirements that the engine must provide in real drive operation and thus to assess the

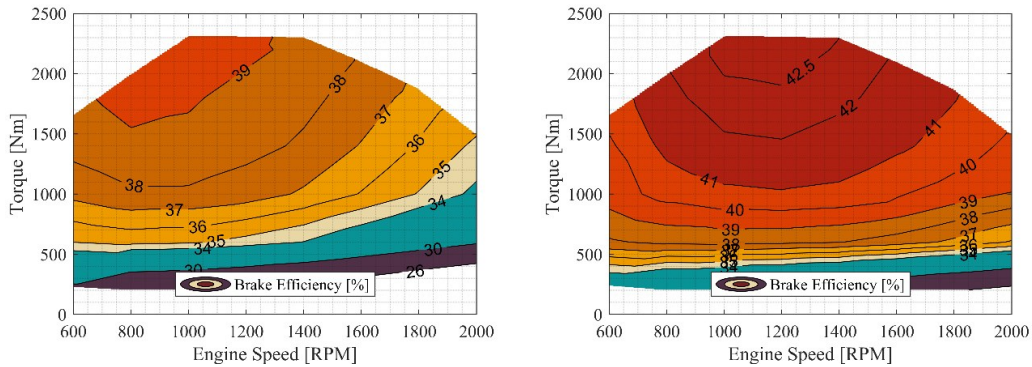


Fig.19 Effective efficiency of CNG engine (left) and C65F35 engine (right)

efficiency and emission potential in real driving conditions. This is to be performed with longitudinal 1D simulations, where the engine models are integrated into powertrain and vehicle models. The air resistance, rolling friction of the tires, vehicle

weight, altitude difference on the track, gear ratio, as well as shifting strategy are all considered in the vehicle model. The selected vehicles and the corresponding driving cycles are listed in **Tab. 4**.

Tab.4 Vehicle and driving cycle

Parameter	Unit	Passenger car	Heavy-duty truck
Vehicle	—	Mercedes Benz E-Class	MAN TGX 18440
Total mass	kg	1 680	40 000
Gearbox	[-]	9	12
Max. torque	N·m	200	2 317
Max. power	k·W	96	354
Driving cycle course	—	Renningen	Stuttgart-Ulm
Distance	k·m	92.8	111
Duration	min	102.8	100
Average velocity	km/h	54.1	66.6

It can be derived from the time portions of operation in Fig. 20 the which load points are of particular significance during the investigated driving cycles. For the passenger car, the area of low to medium speeds at moderate loads are most requested. The full-load portions play a subordinate role here. In the case of long-haul truck, a narrow speed band is frequently run through at varying loads. This results from the mostly stationary speed during highway driving. It is noticeable that full load points with varying speeds are frequently used for acceleration or hill climbing.

The real drive effective efficiency and the NO emissions in mg/km are shown in Fig. 21 for the different fuels and passenger car engine concepts. The gasoline fuel performs best for the base engine concept with approx. 34% effective efficiency. This is due to its higher brake efficiency at part-load thanks to the less throttle losses and shorter combustion

durations, compared with G85F15 or C65F35. Nevertheless, the efficiency disadvantages of both synthetic fuels for the base engine are only moderate and NO emissions have become significantly lower. A NO reduction of 60% is quantified with C65F35. In the case of cost-optimized engine concepts, an efficiency advantage for C65F35 is already achieved with downsizing despite the lack of technologies for higher efficiency. The efficiency level for G85F15 can be maintained with the cost-optimized concept compared to its base variant. For the high-efficiency concepts (HE), the efficiency increases significantly with both synthetic fuels (37.3% for C65F35). The effect of lean combustion can be observed through NO emissions. Especially for C65F35, the NO raw emissions drop to 550 mg/km, correlating to the level of a diesel engine in this segment. A common exhaust aftertreatment concept (NO_x storage catalyst or SCR) makes it possible to keep NO emissions well

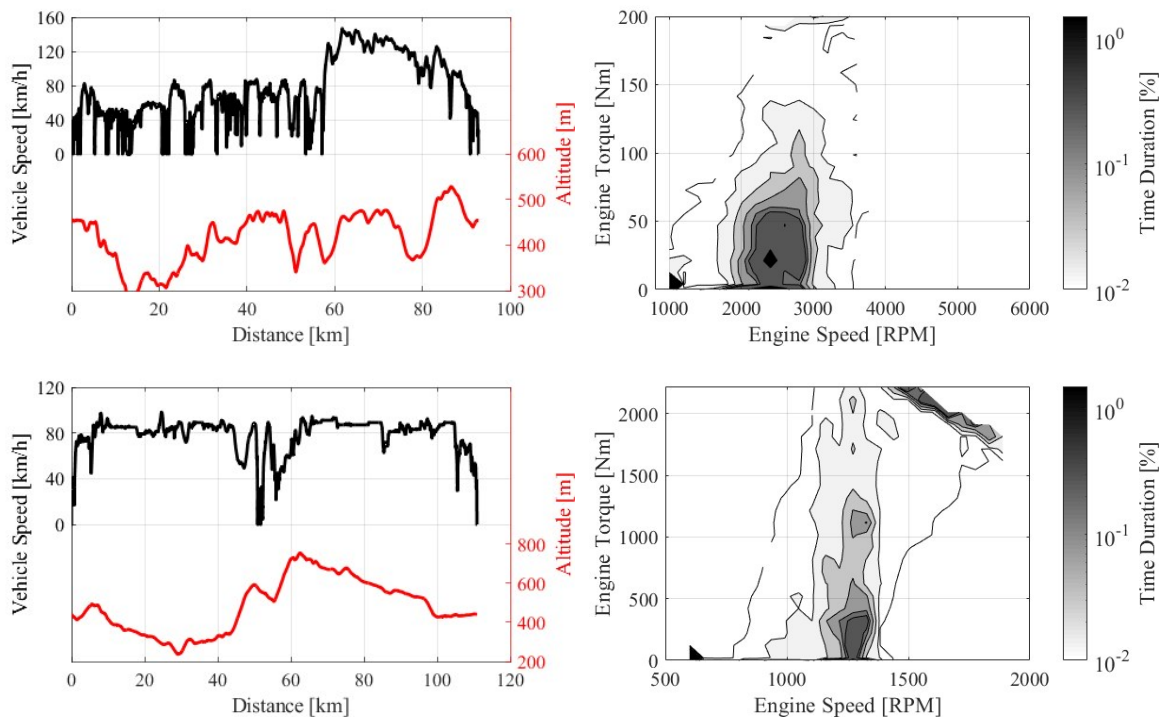


Fig.20 Vehicle speed and altitude of driving cycle and time profile in engine map for passenger car (top) and heavy-duty truck (bottom)

below the Euro 6 limit^[32]. As a bold estimation a pre-chamber spark-plug engine is set up based on the high-efficiency concept of C65F35. The active pre-chamber spark plug serves to increase turbulence and generate multiple ignitions in the combustion chamber, thus reducing burn duration, stabilizing

lean combustion and depressing knock^[33]. These effects were modeled in the simulation by raising the flame speed for about a 35% reduction of burn duration over a wide range of the characteristic map. With this engine concept, an effective efficiency of over 39 % is achieved in the virtual driving cycle.

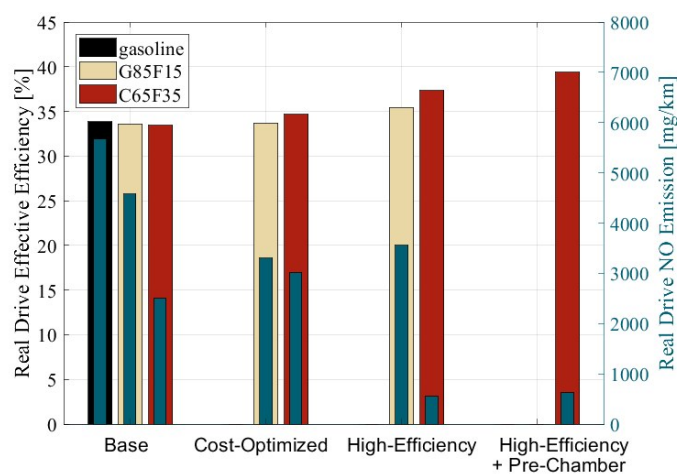


Fig.21 Effective efficiency of passenger car engine concepts in driving cycle with associated NO emissions

Further assessment is made for the four heavy-duty engine concepts. Fig. 22 shows the effective efficiency of the real driving cycle for the four different fuels. While the CNG engine has the lowest

efficiency of 35.5%, the C65F35 cost-optimized concept with an overall efficiency of 37.6 % has come close to the level of the diesel engine (37.7%). The efficiency of C65F35 is achieved with

a significantly less system complexity. The stoichiometric operation avoids complex exhaust aftertreatment system and also leads to lower requirements for boost pressure. The one-stage turbocharging can well meet the boost demand. The highest effective efficiency is realized with OME. The effective average efficiency increases by 3.7 % compared to diesel, while at the same time integral NO_x emissions decrease by 88% and integral particulate raw emissions by 99.98%. The adjustments to the injection system as well as the extended low-pressure EGR path guarantee the best possible efficiencies at real-drive relevant operating points. The low NO and particulate emissions achieved in this way, which are below the EU6 limit value, could be used in the next step to investigate how far the exhaust gas aftertreatment components can be reduced in size and whether part of the exhaust gas aftertreatment can be omitted. This could lower the exhaust backpressure and thus further increase efficiency.

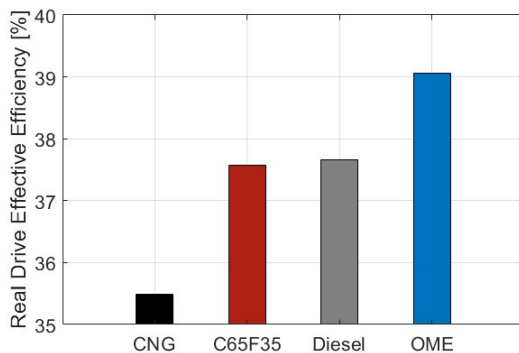


Fig.22 Effective efficiency of heavy-duty truck engine concepts in driving cycle

5 Summary

E-Fuels offer a solution to climate-neutral and low-emission mobility with internal combustion engines. It is possible to adapt the fuels through synthesis to the final applications. This can be done by C1 oxygenates, which have a high potential as alternative diesel and gasoline fuels. The focus of this paper is on the development of 0D/1D simulation models for virtual engine design for synthetic fuels

and to exploit the promising potentials.

In the first step, simulation models were developed for the investigated fuels. For OME fuel, the ignition delay, premixed combustion, and diffusive combustion sub-models were optimized based on the existing diesel combustion model. The NO_x emission model parameters were also optimized to improve the simulation accuracy for low-temperature combustion and high exhaust gas recirculation conditions. Both combustion and emission models are validated with measurement data of diesel and OME. For DMC, MeFo, as well as their blends, the models for calculating charge motion and turbulence, laminar flame speed, knock and NO emission were adapted and validated using 3D-CFD simulations and test bench measurements.

In the second step, adjustments to engine design and operating strategy were made to the synthetic fuels. With OME, higher EGR rates are possible due to the lack of soot-NO_x trade off, which significantly reduces NO emissions. At the same time, lower charge exchange work leads to increased efficiencies. With the aid of additional low-pressure EGR, this efficiency advantage can be demonstrated throughout the entire engine map. At the same time, the injection system must be adapted to compensate for the low calorific value of OME. An increased injection rate through large injector flow can make good use of the rapid mixture preparation and fast burnout of OME to increase efficiency. An OME-fueled engine is designed based on a diesel commercial vehicle engine. For C65F35 as well as G85F15, the necessary engine modifications are on the one hand due to the larger mixture heating value, as a result of which the displacement of the engine can be reduced. Furthermore, the significantly higher knock resistant properties allow more extreme process designs, which also offers great potential for increasing efficiency. In addition, the negative effect of lower laminar flame speeds of DMC und MeFo can be compensated by the concepts for increasing the combustion speed (active pre-chamber ignition, high-turbulence concepts). A cost-optimized and a high-efficiency concept are built for C65F35 and G85F15

respectively, based on a state-of-the-art passenger car gasoline engine.

In the third step, the engine concepts are evaluated in real driving cycles. With G85F15 for passenger car applications, increases in efficiency with lower engine complexity can already be observed. For C65F35, an increase in effective efficiency of up to 10% are possible in real drive for the high-efficiency concept compared with the conventional gasoline engine. The NO emissions in this lean-burn engine concept can be kept below the emission standard with a conventional exhaust aftertreatment system of diesel engine. The great potential of C65F35 is further demonstrated by a cost-optimized engine concept for heavy-duty commercial vehicles. Modified process control makes the spark-ignition engine competitive with conventional diesel concepts while significantly reducing the complexity of exhaust gas aftertreatment and turbocharging. The OME engine shows the highest effective efficiency of over 39% in the real driving cycle and at the same time a reduction of NO raw emissions by 88% and a soot emissions by 99.98%.

References:

- [1] LUMPP B, ROTHE D, PASTÖTTER C, *et al.* Oxymethylether als dieselmotorkraftstoff der zukunft [J]. MTZ - Motortechnische Zeitschrift, 2011, (3): 198.
- [2] MAUS W, JACOB E, HÄRTL M, *et al.* Synthetic fuels—OME1: a potentially sustainable diesel fuel. 35. internationales wiener motorensymposium[M]. Düsseldorf: VDI-Verl, 2014: 325.
- [3] MÜNZ M A, FEILING A, BEIDL C, *et al.* Oxymethylen ether (OME1) as a synthetic low-emission fuel for DI diesel engines [C]// Internationaler Motorenkongress 2016. Wiesbaden: Springer Fachmedien Wiesbaden, 2016: 537. ISBN 978-3-658-12917-0.
- [4] ZHU R, WANG X, MIAO H, *et al.* Effect of dimethoxymethane and exhaust gas recirculation on combustion and emission characteristics of a direct injection diesel engine [J]. Fuel, 2011, 90(5): 1731.
- [5] HÄRTL M, GAUKEL K, PÉLERIN D, *et al.* Oxymethylenether als potenziell CO₂-neutraler Kraftstoff für saubere Dieselmotoren. Teil 1: Motorenuntersuchungen. In Motortechnische Zeitschrift, 2017, 78; S. 52.
- [6] JACOB E, MAUS W, HÄRTL M, *et al.* Oxymethylenether (OME) als potenziell CO₂-neutraler Kraftstoff für saubere Dieselmotoren. Teil 2: Erfüllung des Nachhaltigkeitsanspruchs. In Motortechnische Zeitschrift, 2017, 78; S. 54.
- [7] PACHECO M A, MARSHALL C L. Review of dimethyl carbonate (DMC) manufacture and its characteristics as a fuel additive[J]. Energy & Fuels, 1997, 11; S. 2.
- [8] WEN L B, XIN C Y, YANG S C. The effect of adding dimethyl carbonate (DMC) and ethanol to unleaded gasoline on exhaust emission[J]. Applied Energy, 2010, 87; S. 115.
- [9] KLEZL P, KLEZL P. Fuel for internal combustion engines and use of methyl formate as fuel additive, 1992.
- [10] EICHLER F, DEMMELBAUER-EBNER W, THEOBALD J, *et al.* Der neue EA211 TSI@evo von Volkswagen [C]// 37th International Vienna Motor Symposium. 2016.
- [11] HUNEKE B, KLEESATTEL J, LÖSER S, *et al.* Der neue Sechszylinder-Marinemotor von MAN für Yachten und Arbeitsboote[J]. MTZ Motortech Z, 2016, 77(5): 50.
- [12] LIEBL J. Ladungswechsel im Verbrennungsmotor 2016: Elektrifizierung - Potenziale für den Ladungswechsel - 9. MTZ-Fachtagung' (Springer Fachmedien Wiesbaden, Wiesbaden, 2017).
- [13] LIEBL J. Mercedes-Benz E-Klasse: Entwicklung und Technik des W213' (Springer Vieweg, Wiesbaden, Heidelberg, 2017)
- [14] New MAN TGX 18.400 XLX [EB/OL]. [2022-01-01]. <https://ebook.stuenings-medien.de/flipbook/etc/files/assets/common/downloads/page0018.pdf>.
- [15] 'Sattelzugmaschine MAN TGX 18.440 (400-480) BLS', <https://www.europa-lkw.de/technische-daten-modell/man-tgx-18-440-4x2-bls-efficient-line>, accessed January, 2022.
- [16] Barba, C.: 'Erarbeitung von Verbrennungskennwerten aus Indizierdaten zur verbesserten Prognose und rechnerischen Simulation des Verbrennungsablaufes bei Pkw-DE-Dieselmotoren mit Common-Rail-Einspritzung', ETH Zurich, 2001.
- [17] FKFS: 'Bedienungsanleitung UserCylinder Version 2.7.2' (2021).
- [18] Rether, D., Schmid, A., Grill, M., Bargende, M.: 'Quasidimensionale Simulation der Dieselerverbrennung mit vor- und Nacheinspritzungen', MTZ Motortech Z, 2010, 71, (10), pp. 742 - 748.
- [19] Reif, K.: 'Dieselmotor-Management: Systeme, Komponenten, Steuerung und Regelung' (Springer Fachmedien Wiesbaden GmbH, Wiesbaden, 2020, 6th edn.).
- [20] Kožuch, P.: 'Ein phänomenologisches Modell zur kombinierten Stickoxid- und Rußberechnung bei direkteinspritzenden Dieselmotoren' (Universität Stuttgart, 2004).
- [21] Kaal, B.; Grill, M.; Bargende, M.: Transient Simulation of Nitrogen Oxide Emissions of CI Engines. SAE Paper 2016-01-1002, 2016.
- [22] Hann, S., Grill, M., Bargende, M., "A quasi-dimensional si combustion model predicting the effects of changing fuel, air-fuel-ratio, egr and water injection," in SAE Technical Paper

- 2020.
- [23] Grill, M., Billinger, T., and Bargende, M., "Quasi-Dimensional Modeling of Spark Ignition Engine Combustion with Variable Valve Train," SAE Technical Paper 2006-01-1107, 2006, <https://doi.org/10.4271/2006-01-1107>.
- [24] Fritsch, S., Fasse, S., Yang, Q., Grill, M., Bargende, M.: 'A Quasi-Dimensional Charge Motion and Turbulence Model for Spark Injection Engines with Fully Variable Valve Train and Direct Fuel Injection', in Liebl, J. (Ed.): 'Experten-Forum Powertrain: Ladungswechsel und Emissionierung 2019' (Springer Fachmedien Wiesbaden, Wiesbaden, 2020), pp. 24 - 39.
- [25] Hann, S.: 'A Quasi-Dimensional SI Burn Rate Model for Carbon-Neutral Fuels' (Springer Fachmedien Wiesbaden; Imprint Springer Vieweg, Wiesbaden, 2021, 1st edn.)
- [26] Cai, L., Ramalingam, A., Minwegen, H., Alexander Heufer, K., Pitsch, H.: 'Impact of exhaust gas recirculation on ignition delay times of gasoline fuel: An experimental and modeling study', Proceedings of the Combustion Institute, 2019, 37, (1), pp. 639 - 647.
- [27] Blochum S., Fellner F., Mühlthaler M., Härtl M., Wachtmeister G., Yoneya N., Sauerland H.: Comparison of Promising Sustainable C1-Fuels Methanol, Dimethyl Carbonate, and Methyl Formate in a DISI Single-Cylinder Light Vehicle Gasoline Engine. SAE Powertrains, Fuels & Lubricants Digital Summit, 2021.
- [28] Blochum, S.; Gadomski, B.; Retzlaff, M.; Thamm, F.; Kraus, Ch.; Härtl, M.; Gelhausen, R.; Hoppe, St.; Wachtmeister, G.: Potential Analysis of a DMC/MeFo Mixture in a DISI Single and Multi-Cylinder Light Vehicle Gasoline Engine. SAE International, 2021.
- [29] Doombos, G., Hemdal, S., Denbratt, I., & Dahl, D. (2018). Knock Phenomena under Very Lean Conditions in Gasoline Powered SI-Engines. SAE International Journal of Engines, 11 (1), 39 - 54. <https://www.jstor.org/stable/26562340>.
- [30] Weller, R., Bauer, H., Braun, T., et al.: 'Einfluss des Ladungswechsels auf das Emissionskonzept des neuen 4-Zylinder-Dieselmotors (OM654) von Mercedes-Benz'. Ladungswechsel im Verbrennungsmotor, Stuttgart.
- [31] Yang, K., Grill, M., Bargende, M.: 'A Simulation Study of Optimal Integration of a Rankine Cycle Based Waste Heat Recovery System into the Cooling System of a Long-Haul Heavy Duty Truck'. International Powertrains, Fuels & Lubricants Meeting, SEP. 17, 2018.
- [32] Demuyneck, J., Bosteels, D., Bunar, F. and Spitta, J.: "Diesel-pkw mit extrem niedrigem nox-niveau im realfahrbetrieb," MTZ - Motortechnische Zeitschrift, no. 1, pp. 42 - 47, 2020.
- [33] Sens, M. and Binder, E.: "Vorkammerzündung als Schlüsseltechnologie für den zukünftigen antriebsmix," MTZ - Motortechnische Zeitschrift, no. 2, 2019.
- [34] Richter, G., Zellbeck, H.: 'OME als Kraftstoffersatz im Pkw-Dieselmotor', MTZ Motortech Z, 2017, 78, (12), pp. 66 - 73.
- [35] FVV, ed., ICE2025+: Ultimate System Efficiency: Limits of overall SI engine efficiency in hybridized powertrains: Project no. 1307. 2020.